Available online at www.sciencedirect.com
ScienceDirect
Journal of Nuclear Materials 360 (2007) 222–230
journal of nuclear materials
www.elsevier.com/locate/jnucmat

Influence of ageing heat treatment on alloy A-286 microstructure and stress corrosion cracking behaviour in PWR primary water

M. Savoie [a,b], C. Esnouf [c], L. Fournier [a], D. Delafosse [b,*]

[a] Commissariat à l'Energie Atomique, CEA Saclay, DMN/SEMI/LCMI, 91191 Gif-Sur-Yvette, France
[b] Ecole Nationale des Mines de Saint-Etienne, Centre Science des Matériaux et des Structures, SMS Division, UMR CNRS 5146, 158 cours Fauriel, 42023 Saint-Etienne cedex 02, France
[c] Groupe d'Etude de Metallurgie Physique et de Physique des Matériaux, INSA Lyon, 69621 Villeurbanne, France

Received 15 June 2006; accepted 11 October 2006

Abstract

The influence of ageing heat treatment on alloy A-286 microstructure and stress corrosion cracking behaviour in simulated Pressurized Water Reactor (PWR) primary water has been investigated. A-286 microstructure was characterized by transmission electron microscopy for ageing heat treatments at 670 °C and 720 °C for durations ranging from 5 h to 100 h. Spherical γ' phase with mean diameters ranging from 4.6 to 9.6 nm and densities ranging from $8.5 \times 10^{22}\ m^{-3}$ to $2 \times 10^{23}\ m^{-3}$ were measured. Results suggest that both the γ' phase mean diameter and density quickly saturate with time for ageing heat treatment at 720 °C while the γ' mean diameter increases significantly up to 100 h for ageing heat treatment at 670 °C. Grain boundary η phase precipitates were systematically observed for ageing heat treatment at 720 °C even for short ageing periods. In contrast, no grain boundary η phase precipitates were observed for ageing heat treatments at 670 °C except after 100 h. Hardening by γ' precipitation was well described by the dispersed barrier hardening model with a γ' barrier strength of 0.23. Stress corrosion cracking behaviour of A-286 was investigated by means of constant elongation rate tensile tests at $1.5 \times 10^{-7}\ s^{-1}$ in simulated PWR primary water at 320 °C and 360 °C. In all cases, initiation was transgranular while propagation was intergranular. Grain boundary η phase precipitates were found to have no significant effect on stress corrosion cracking. In contrast, yield strength and to a lesser extent temperature were found to have significant influences on A-286 susceptibility to stress corrosion cracking.

1. Introduction

Precipitation-hardening austenitic stainless steel A-286 is widely used in the gas turbine industry for its high strength and corrosion resistance. Since it also has a thermal coefficient of expansion comparable to type 304 SS, it is also used for reactor vessel internals bolting applications in the nuclear industry [1]. Several A-286 reactor vessel internals bolts failures were reported during PWR in-service inspections in the early 1980s [1,2]. The subsequent extensive evaluation program identified intergranular

* Corresponding author. Tel.: +33 4 77 42 02 98; fax: +33 4 77 42 01 57.
E-mail address: david.delafosse@emse.fr (D. Delafosse).

0022-3115/$ - see front matter © 2006 Elsevier B.V. All rights reserved.
doi:10.1016/j.jnucmat.2006.10.003

stress corrosion cracking (IGSCC) as the degradation mechanism and recommended to operate bolts at stress levels below the material's yield stress [1,2]. However, the effect of heat treatment and metallurgical structure on IGSCC has received little attention for A-286 in comparison to other precipitation-hardening NiFeCr alloys 718 and X-750 also used in the nuclear industry for bolts, springs, beams and pins [3,4]. The aim of this study was therefore to gain insights into the influence of microstructure on A-286 SCC behaviour in simulated PWR primary water.

A-286 is strengthened by the ordered cubic γ' $Ni_3(Ti, Al)$ phase [5]. However it is also susceptible to the formation of the stable HCP η Ni_3Ti phase during the ageing heat treatment. The effect of ageing heat treatment at 670 °C and 720 °C for durations ranging from 5 h to 100 h on both γ' and η phase precipitation was therefore first carefully investigated by Transmission Electron Microscopy (TEM). On the basis of these results the effect of the same ageing heat treatment on A-286 SCC susceptibility was studied by means of constant elongation rate tensile (CERT) tests in simulated PWR primary water at 320 °C and 360 °C.

2. Experimental procedure

The chemical composition of the A-286 used in this work is given in Table 1. All specimens were machined out of a 12.5 mm diameter rod provided by UGITECH and encapsulated under primary vacuum in quartz tubes for solution annealing and ageing heat treatments. Solution annealing was carried out at 930 °C for 1 h and followed by water quenching.

Grain size was determined after mechanical polishing with wet SiC abrasive paper down to 1 μm roughness and chemical etching in a 30 cc HCl, 30 cc HNO_3, 20 cc CH_3COOH and 20 cc H_2O solution for 30 s. An average grain size of 6 μm was measured.

TEM thin foils were prepared using a Tenupol twin jet electropolishing unit with a 70% ethanol, 20% *n*-butyl alcohol and 10% perchloric acid electrolyte at −20 °C and 70 V. Microstructures were characterized using a Tecnai FEI transmission electron microscope operating at 300 kV and equipped with a Gatan CCD digital camera. γ' precipitates were imaged by means of the dark field technique using a 5 μm diameter objective aperture and the superlattice reflexion $(1\,0\,0)_{\gamma'}$ of the $\langle 1\,1\,0\rangle$ zone axis. Thin foil thicknesses were determined using thickness fringes along a grain boundary.

Smooth tensile test specimens with a 4 mm diameter and a 36 mm gauge length were used for SCC testing. All specimens were mechanically polished with SiC paper down to grit 4000 and rinsed with ethanol prior to SCC testing. In order to determine the effect of the cold-worked layer created by mechanical polishing on A-286 SCC behaviour, a single specimen was also electropolished at 10 V during 1 min with a 45% methanol, 45% *n*-butyl alcohol and 10% perchloric acid solution at room temperature. CERT tests were performed at $1.5 \times 10^{-7}\,s^{-1}$ in simulated PWR primary water (1000 ppm of boric acid and 2 ppm of lithium hydroxide) at 320 °C and 360 °C in a 0.88 l austenitic stainless steel static autoclave. All tests were conducted with a 30 cc/kg H_2O dissolved hydrogen concentration controlled with a Pd/Ag probe. The engineering stress–strain curves obtained were post-processed by linearly fitting the elastic part to a Young's modulus of 200 GPa. Analysis of both the fracture and the side surfaces of specimens after CERT testing was carried out using a field emission gun (FEG) – scanning electron microscope (SEM). Prior to SEM examination specimens were ultrasonically cleaned first for 2 h in a 20 cc hydrochloric acid and 80 cc water solution with 2 g hexamethylenetetramine inhibitor and then in acetone for 5 min in order to remove the oxide layer formed during CERT testing in high temperature water.

3. Results

3.1. Microstructure

As mentioned earlier, γ' and η phase precipitation for ageing heat treatment at 670 °C and 720 °C up to 100 h was first carefully investigated

Table 1
Chemical composition of A-286 (in wt%)

Fe	Ni	Cr	Ti	Mn	Mo	V	Al	Cu	Si	Nb	Co	C	P	S
Bal.	25	14.1	1.97	1.65	1.18	0.29	0.18	0.14	0.1	0.08	0.08	0.04	0.02	<0.001

by TEM in this study. Results of this characterisation are described below.

3.1.1. γ' phase

The γ' mean diameter, volume fraction and density measured after ageing for 50 and 100 h at 670 °C, and for 5, 16, 24 and 100 h at 720 °C are summarized in Table 2. Between 192 and 1066 precipitates in 3–5 different areas of a single TEM foil were analysed for each ageing condition. Thin foils thickness ranged between 30 and 110 nm. A dark field TEM micrograph of γ' precipitation for the 16 h at 720 °C ageing heat treatment is displayed in Fig. 1. Size distribution histograms for γ' precipitates are shown in Fig. 2 for all the investigated ageing heat treatments. It should be mentioned here that γ' precipitates were too small to be imaged by TEM for ageing at 670 °C for 24 h. The evolution of the γ' precipitate density and mean diameter as a function of ageing time are shown in Figs. 3 and 4, respectively.

Mean diameters ranged from 4.6 to 9.6 nm. The mean diameter increased with short ageing times at 720 °C, reached a maximum at 16 h, then decreased for 24 h and seemed to saturate for ageing times up to 100 h. In contrast, mean diameter was still increasing with ageing time up to 100 h at 670 °C. The mean diameter measured in this study after ageing at 720 °C for 5 h is consistent with the value reported by Thompson [6] for a slightly higher ageing duration at the same temperature. The mean diameter measured in this study after ageing at 720 °C for 16 h is also in excellent agreement with the values reported by Thompson [6] and De Cicco [7] for the same ageing conditions.

Densities ranged from $8.5\times10^{22}\,m^{-3}$ to $2\times10^{23}\,m^{-3}$ and seemed to saturate around $10^{23}\,m^{-3}$ to $2\times10^{23}\,m^{-3}$ with ageing time at both 670 °C and 720 °C.

3.1.2. η phase

The results of η phase TEM observations after ageing for 24, 50 and 100 h at 670 °C, and 5, 16, 24 and 100 h at 720 °C are summarized in Table 3. About 100 grain boundaries in 2 different TEM foils were observed for each ageing condition. As illus-

Table 2
Summary of γ' mean diameter, volume fraction and density measurements for A-286 with various ageing heat treatments

Ageing heat treatment	# of TEM foil observed	# of grains observed	# of precipitates measured	Mean γ' diameter (nm)	γ Volume fraction (%)	γ density (m)
670 °C for 50 h	1	3	192	4.6	0.8	1.6×10^{23}
670 °C for 100 h	1	3	271	6.2	2.5	2×10^{23}
720 °C for 5 h	1	4	465	6.4	1.3	9.3×10^{22}
720 °C for 16 h	1	5	1066	9.6	3.9	8.5×10^{22}
720 °C for 24 h	1	3	246	7.2	2.6	1.3×10^{23}
720 °C for 100 h	1	5	427	7.6	3.3	1.4×10^{23}

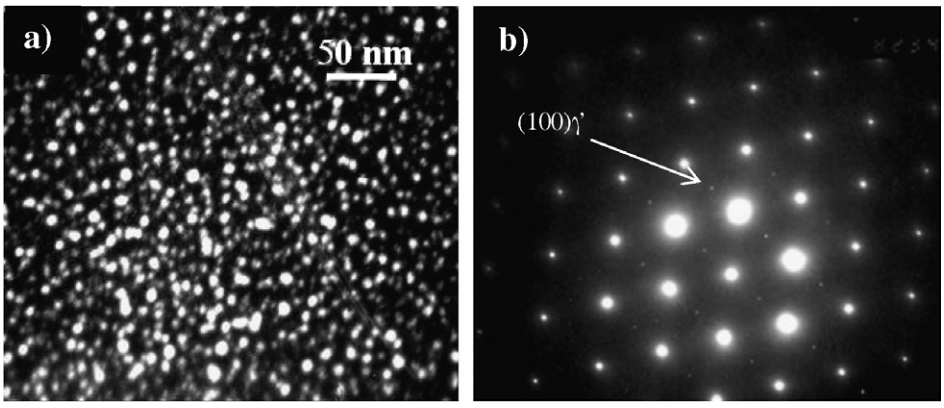

Fig. 1. (a) Dark-field TEM micrograph showing γ' precipitates in the specimen aged 16 h at 720 °C. The associated diffraction pattern is shown in (b). The precipitates were imaged using $(100)_{\gamma'}$ superlattice reflexion (indicated by an arrow) in zone axis $\langle 110\rangle$.

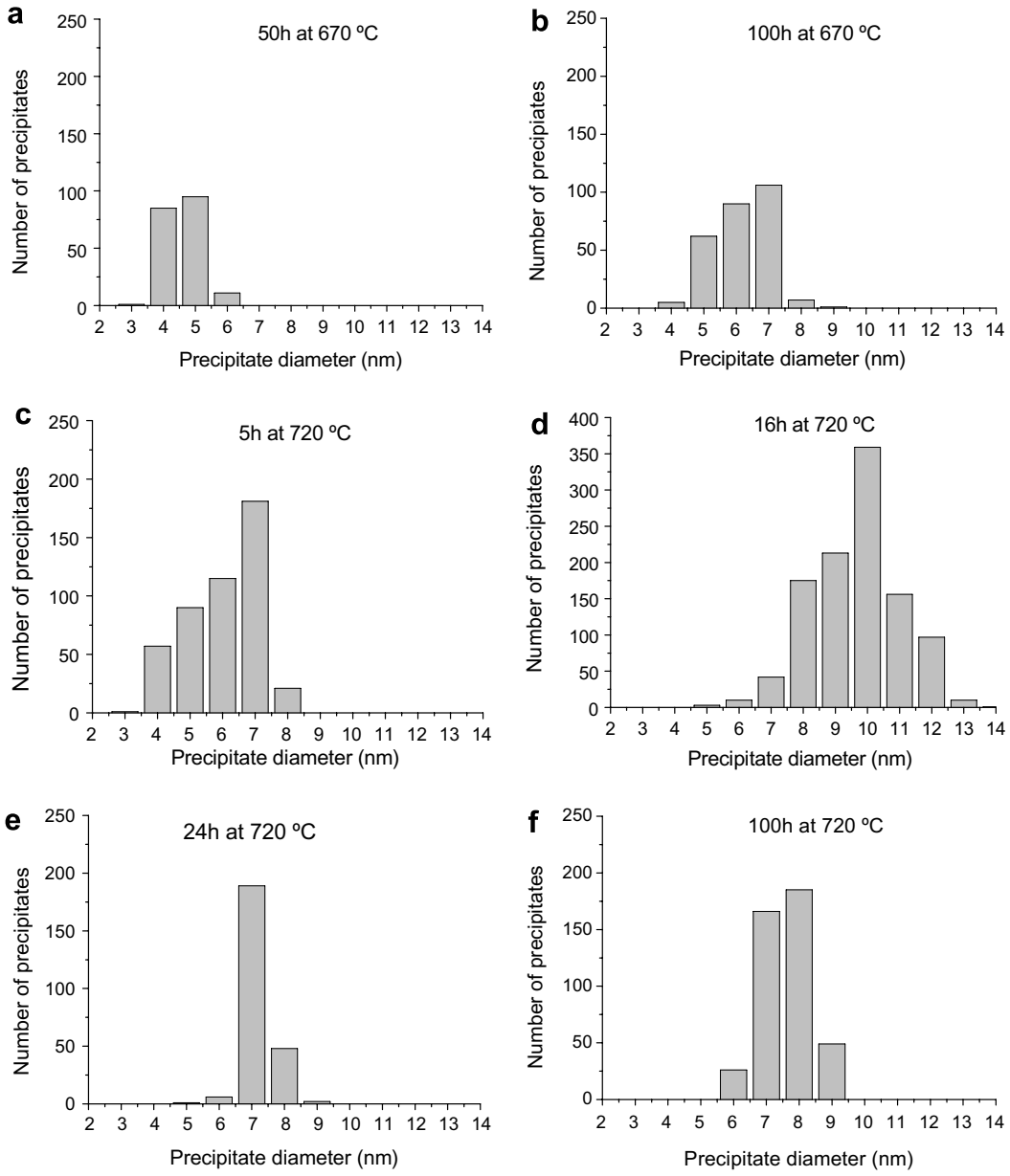

Fig. 2. γ' precipitate size distribution in alloy A-286 aged for (a) 50 h and (b) 100 h at 670 °C and for (c) 5 h, (d) 16 h, (e) 24 h and (f) 100 h at 720 °C.

trated in Fig. 5, η phase in the form of discs or platelets were found to decorate grain boundaries. The fraction of grain boundaries decorated by η phase is displayed in Table 3 with a distinction made between grain boundaries with disc η phase and grain boundaries with platelets of η phase. In good agreement with results from Brooks et al. [8], grain boundary η phase precipitates were systematically observed for ageing heat treatment at 720 °C even after short ageing periods. In contrast, no grain boundary η phase precipitates were observed for ageing heat treatment at 670 °C except after 100 h ageing.

3.2. Precipitation-induced hardening

Precipitation-induced hardening was quantified by subtracting the yield stress value measured for solution annealed A-286 during tensile testing at

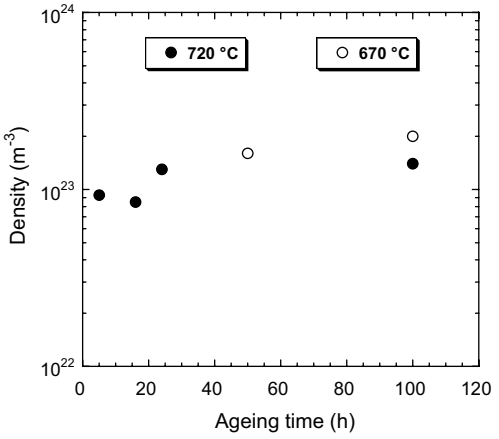

Fig. 3. γ' density evolution as a function of ageing time at 670 °C and 720 °C.

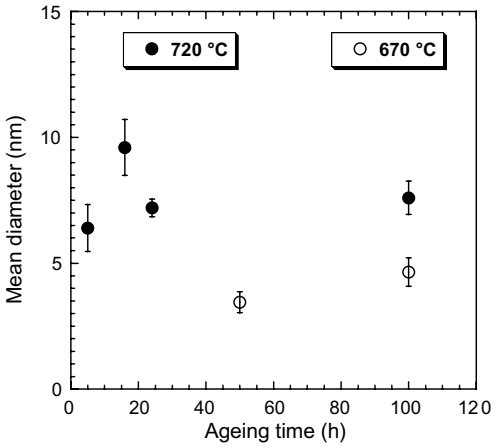

Fig. 4. γ' mean diameter evolution as a function of ageing time at 670 °C and 720 °C.

360 °C from the yield stress value measured after CERT testing at 1.5×10^{-7} s^{-1} in simulated primary water at 360 °C for ageing heat treatments at 670 °C for 50 h and 100 h and at 720 °C for 16 h and 100 h. These calculated precipitation-induced increments in yield stress ($\Delta\sigma$) are listed in Table 4 together with the mean γ' diameter and density reported in the previous section for the corresponding ageing heat treatment. $\Delta\sigma$ and γ' precipitate sizes and densities were used to calculate the γ' barrier strength using the dispersed barrier hardening model:

$$\Delta\sigma = M\alpha\mu b(Nd)^{1/2}, \quad (1)$$

where $\Delta\sigma$ is the yield strength increase, M is the Taylor factor (3.06 for FCC metals [9]), α is the barrier strength, μ is the shear modulus (75.8 GPa for A-286 alloy [10]), b is the Burgers vector (0.25 nm), N is the barrier density and d is the barrier size. γ' barrier strength values calculated for ageing heat treatment at 670 °C for 50 h and 100 h and at 720 °C for 16 h and 100 h are listed in Table 4. All values are in good agreement and lie around 0.23.

3.3. Stress corrosion cracking

The results of the CERT tests performed in simulated PWR primary water at 320 and 360 °C on specimens aged at 670 °C for 24 h, 50 h and 100 h and at 720 °C for 16 h and 100 h are summarized in Table 5. The yield strength, ultimate tensile strength, strain to failure, percentage of 'brittle' cracking on fracture surface, and total crack length on side surface are tabulated for each specimen. SEM micrographs of the fracture surfaces of specimens aged 50 h at 670 °C and 100 h at 720 °C and strained in PWR primary water at 320 °C and 360 °C are displayed in Fig. 6.

The specimen aged at 670 °C for 24 h and strained at 320 °C in simulated PWR primary water exhibited a fully ductile failure mode. It exhibited the largest strain to failure (26%) and did not display any cracks on its side-surface. All the other tested specimens were susceptible to SCC. In all

Table 3
Summary of η phase TEM observations for A-286 with various ageing heat treatments

Ageing heat treatment	# of TEM foil observed	# of GB observed	% of GB with disc η phase	% of GB with platelets η phase	Total GB with η phase (%)
670 °C for 24 h	2	100	0	0	0
670 °C for 50 h	2	100	0	0	0
670 °C for 100 h	2	100	24	6	30
720 °C for 5 h	2	100	58	28	86
720 °C for 16 h	2	100	40	50	90
720 °C for 24 h	2	100	40	52	92
720 °C for 100 h	2	100	18	62	80

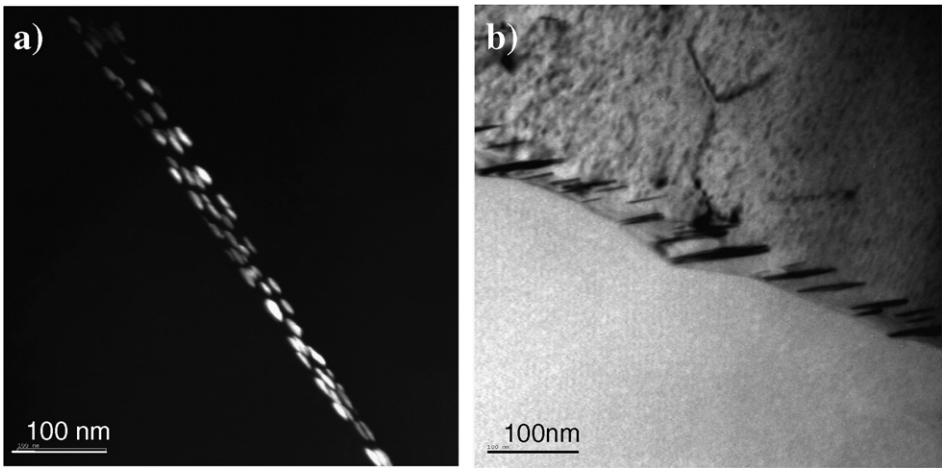

Fig. 5. TEM (a) dark field micrograph of grain boundary discs of η phase in A-286 alloy aged 5 h at 720 °C and (b) bright field micrograph of grain boundary η phase platelets in A-286 aged 16 h at 720 °C.

Table 4
Summary of γ′ barrier strength calculated for A-286 with various ageing heat treatment using the dispersed barrier hardening model and γ′ mean diameters and densities measured by TEM

Ageing heat treatment	Mean γ′ diameter (nm)	γ density (m^{-3})	Δσ (MPa) from CERT tests at 360 °C	γ′ α barrier strength
670 °C for 50 h	4.6	1.6×10^{23}	402	0.25
670 °C for 100 h	6.2	2×10^{23}	503	0.24
720 °C for 16 h	9.6	8.5×10^{22}	365	0.22
720 °C for 100 h	7.6	1.4×10^{23}	393	0.21

Table 5
Summary of SCC results (YS, UTS, Strain to failure, % of brittle TG and IG cracking on the fracture surface, and total crack length on side surface) obtained after CERT testing at 1.5×10^{-7} s^{-1} in simulated PWR primary water for A-286 with various ageing heat treatment

Ageing heat treatment	Test temperature (°C)	YS (MPa)	UTS (MPa)	Strain to failure (%)	% brittle TG IG cracking on fracture surface	Total crack length on side surface (μm)
670 °C for 24 h	320	558	917	26	0	0
670 °C for 50 h	320	665	1032	22	9	9225
670 °C for 24 h	360	570	937	23	3	1250
670 °C for 50 h	360	675	978	14	19.5	5243
670 °C for 100 h	360	776	936	6.5	24	15108
720 °C for 16 h	360	638	993	17	9	702
720 °C for 100 h	360	670	912	12.5	11	9792

the latter cases, cracks initiated and propagated for a few tens of μm in a transgranular (TG) mode, and then propagated in an intergranular (IG) mode. The possible influence of the cold-worked layer resulting from mechanical surface polishing on the TG initiation mode was investigated by means of a specific CERT test in the same conditions on a specimen aged at 720 °C for 16 h and then was electropolished before testing. Initiation and first few tens of μm of propagation remained transgranular suggesting that cold-worked layer resulting from mechanical surface polishing is not responsible for TG initiation.

Serrations on the stress–elongation curves were observed for all conditions of ageing after CERT

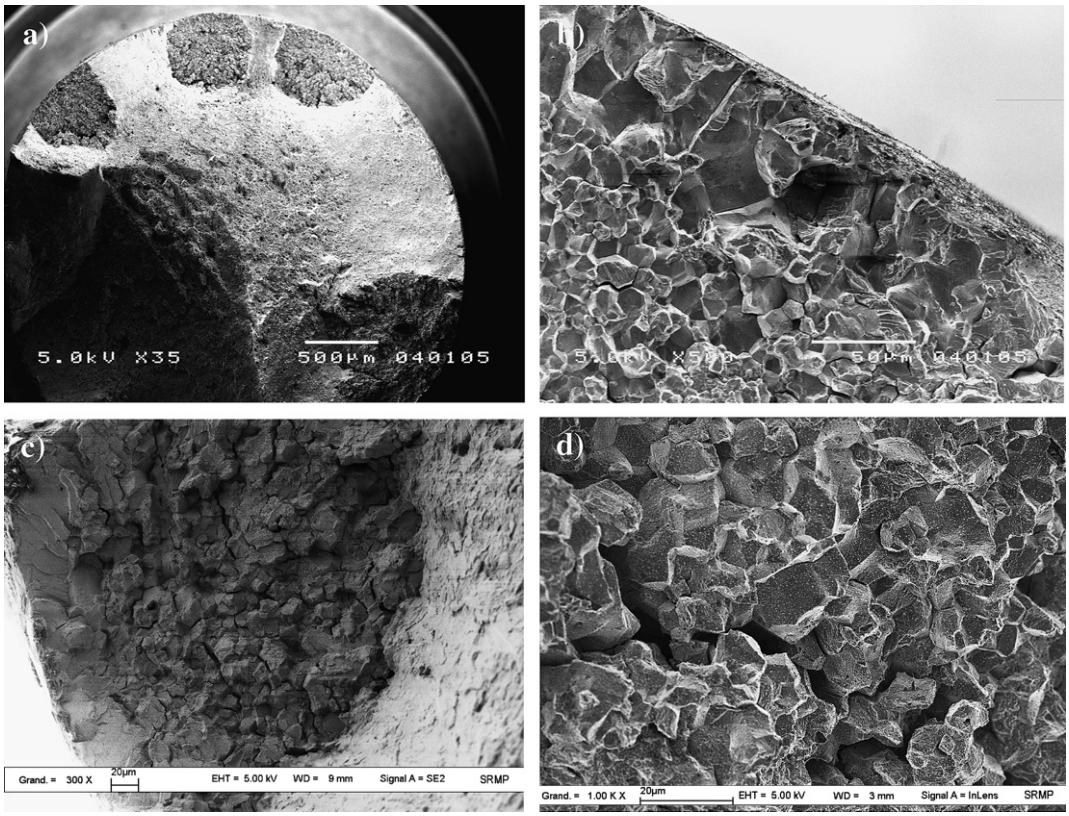

Fig. 6. SEM micrographs of the fracture surfaces of specimens aged (a, b) 50 h at 670 °C and SCC tested at 360 °C, (c) 100 h at 720 °C and SCC tested at 360 °C and (d) 50 h at 670 °C and SCC tested at 320 °C showing TG initiation and IG propagation.

testing in simulated PWR primary water. It is well known that stainless steels are prone to plastic instabilities due to the Portevin–Le Chatelier (PLC) effect in the temperature and strain rate regime investigated in this study [11–13]. It is also well established that PLC effect domain is a sub-domain of dynamic strain aging (DSA) where the strain rate sensitivity of the flow stress (SRS= $\Delta\sigma/\Delta \ln \dot{\varepsilon}$) is negative [14,15]. A specific tensile test was therefore performed with a strain rate jump from 1×10^{-4} s^{-1} to 1.5×10^{-7} s^{-1} at 6% of plastic strain at 360 °C in order to determine the SRS of the flow stress of A-286. A value of −4.25 MPa was measured, demonstrating that observed serrations were indeed due to the PLC effect. Several authors have recently investigated possible interactions between DSA and PLC effect on environmentally assisted cracking (EAC) phenomena [16–18]. In this work, the PLC effect was observed for all specimens strained at 1.5×10^{-7} s^{-1} independently of the ageing heat treatment while SCC was not observed for all specimens and the susceptibility varied with heat treatment. This suggests that PLC effect does not play a significant role in A-286 SCC behaviour in PWR primary water.

Test temperature was found to significantly increase A-286 SCC susceptibility in simulated PWR primary water. As already mentioned, the specimen aged at 670 °C for 24 h was not susceptible to SCC at 320 °C. In contrast, the specimen aged in the same condition exhibited 3% brittle cracking on its fracture surface after CERT testing at 360 °C. For the specimens aged at 670 °C for 50 h, increasing the test temperature from 320 °C to 360 °C led to an increase in the percentage of brittle cracking on the fracture surface from 9% to 19.5%.

Ageing conditions were also found to have a strong impact, probably via the yield stress, on A-286 SCC susceptibility in simulated PWR primary water. The effect of the yield strength on SCC is illustrated in Fig. 7. Clearly, an increase in the yield strength results in a significant increase in susceptibility of the material to SCC. In contrast, grain boundary η phase was not found to play a significant role on A-286 SCC.

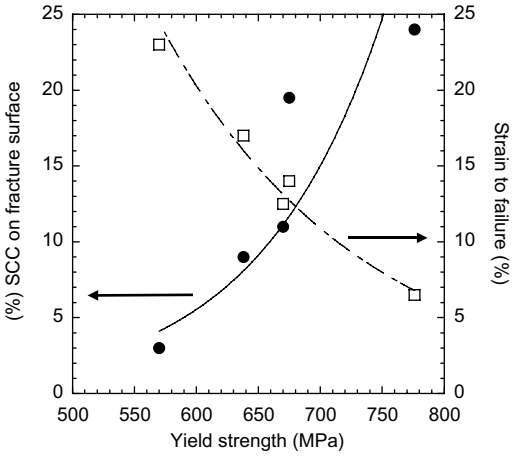

Fig. 7. Evolution of the percentage of 'brittle' cracking on fracture surface and strain to failure as a function of yield strength in alloy A-286 strained at 1.5×10^{-7} s^{-1} in PWR primary water at 360 °C.

4. Discussion

This study of different ageing heat treatment allows discussion of the effect of yield strength and η phase precipitation on A-286 SCC behaviour in simulated PWR primary water.

4.1. Influence of yield strength

The evolution of the percentage of brittle cracking on the fracture surface is plotted together with the evolution of strain to failure as a function of yield strength in Fig. 7. Increasing the yield strength led to a significant increase in the percentage of brittle cracking on the fracture surface and a concomitant decrease in strain to failure. Also, increasing the yield strength is seen to lead to a significant increase in the total crack length on side surface (Table 5). These results clearly demonstrate the important role of the yield strength in the SCC behaviour of A-286 in simulated PWR primary water.

This result is in good agreement with the strong influence of yield strength on crack growth rate of stainless steels reported by Andresen et al. [19] in high purity water with 95 and 1580 ppb of hydrogen at a stress intensity factor around 30 $MPa\sqrt{m}$.

4.2. Influence of η phase

Precipitation strengthened alloys are known to be susceptible to coherent hardening phase transformation into HCP phases that may play a detrimental role in EAC phenomena [20]. In precipitation hardened nickel-based alloy 718, γ″ transformation into δ phase is well documented and Miglin et al. [21] suggested a correlation between the presence of grain boundary δ phase and the SCC susceptibility in simulated PWR primary water.

The results obtained in this study do not suggest any correlation between the amount of grain boundary coverage by η phase and SCC susceptibility. Moreover, as shown in Table 5, specimens aged at 670 °C for 50 h and at 720 °C for 100 h exhibited similar yield strengths and similar susceptibility to SCC. In contrast, as shown in Table 3, the specimen aged at 670 °C for 50 h did not contain any GB η phase while the specimen aged at 720 °C for 100 h had 80% of GB's decorated with η phase, suggesting that η phase does not play a significant role in A-286 SCC in PWR primary water.

5. Conclusions

The influence of ageing heat treatments at 670 °C and 720 °C for durations ranging from 5 h to 100 h on A-286 microstructure and its SCC behaviour in simulated PWR primary water was investigated in this study. Results can be summarized as follows:

1. Spherical γ′ precipitation occurs in the early stage of ageing. Ageing at 670 °C leads to γ′ precipitates that increase in size up to 100 h. In contrast, both γ′ phase size and density quickly saturate after 20 h of ageing heat treatment at 720 °C.
2. γ′ precipitation-induced hardening is well described using the dispersed barrier hardening model with a γ′ barrier strength value of 0.23.
3. Grain boundary η phase precipitation systematically occurs for ageing heat treatment at 720 °C even for short ageing periods. In contrast, no grain boundary η phase precipitation occurs for ageing heat treatment at 670 °C until 100 h ageing.
4. A-286 is susceptible to SCC when strained at 1.5×10^{-7} s^{-1} in PWR primary water at 320 °C and 360 °C with the exception of ageing heat treatment at 670 °C for 24 h and CERT testing at 320 °C. In all cases, initiation is transgranular while propagation is intergranular. A-286 SCC susceptibility correlates well with yield strength. Both the amount of 'brittle' cracking on the fracture surface as well as the total crack length observed on the side surface increase significantly with increasing yield strength.

5. An increase in the test temperature from 320 °C to 360 °C also increases A-286 SCC susceptibility.
6. Grain boundary η phase is shown to have no significant detrimental effect on SCC susceptibility of A-286 in simulated PWR primary water.

Acknowledgments

Financial support was provided by CEA/DSOE-RB. The authors gratefully acknowledge researchers from CEA/SCCME for their help in conducting CERT testing in simulated PWR primary water and researchers from CEA/SRMP for SEM-FEG examinations after SCC testing.

References

[1] R.S. Piascik, K.E. Moore, Nucl. Technol. 75 (1986) 370.
[2] J.B. Hall, S. Fyfitch, K.E. Moore, in: Proceedings of the 11th International Conference on Environmental Degradation of Materials in Nuclear Power Systems – Water Reactors, Stevenson, Washington, August 10–14, 2003 (NACE), p. 208.
[3] M.T. Miglin, H.A. Domain, J. Mater. Eng. 9 (2) (1987) 113.
[4] I.L.W. Wilson, T.R. Mager, Corrosion 42 (6) (1986) 352.
[5] K. Kusabiraki, Y. Takasawa, T. Ooka, ISIJ Int. 35 (5) (1995) 542.
[6] A.W. Thompson, J.A. Brooks, Acta Metal. 30 (1982) 2197.
[7] H. De Cicco, M.I. Luppo, L.M. Gribaudo, J. Ovejero-Garcia, Mater. Charact. 52 (2004) 85.
[8] J.A. Brooks, A.W. Thompson, Metall. Trans. 24A (1993) 1983.
[9] R.E. Stoller, S.J. Zinkle, J. Nucl. Mater. 283–287 (2000) 349.
[10] H.M. Ledbetter, W.F. Weston, E.R. Naimon, J. Appl. Phys. 469 (1975) 3855.
[11] R.W. Hayes, W.C. Hayes, Acta Metall. 30 (1982) 1295.
[12] W. Chen, M.C. Chaturvedi, Mater. Sci. Eng. A 229 (1997) 163.
[13] A.A. Abduluyahed, K. Rozniatowski, K.J. Kurzydlowski, Scripta Metall. Mater. 33 (9) (1995) 1489.
[14] L.P. Kubin, Y. Estrin, Acta Metall. Mater. 38 (5) (1990) 697.
[15] A. Van Den Beukel, Acta Metall. 28 (1979) 965.
[16] L. Fournier, D. Delafosse, T. Magnin, Mater. Sci. Eng. A 316 (2001) 166.
[17] V. Garat, J.M. Cloué, B. Viguier, E. Andrieu, in: Proceedings of the Sixth International Special Emphasis Symposium on Superalloy 718, 625, 706 and Derivatives, Pittsburgh, Pennsylvania, October 2–5, 2005.
[18] U. Ehrnsten, M. Ivanchenko, V. Nevdacha, Y. Yagozinskyy, A. Toivonen, H. Hanninen, in: Proceedings of Eurocorrosion Conference 2004, Nice, September 12–16, 2004.
[19] P.L. Andresen, M.M. Morra, W.C. Catlin, in: Proceedings of NACE Corrosion 2004, March 28–April 1, New Orleans, Louisiana, 2004 (NACE) Paper No. 04678.
[20] E.E. Brown, D.R. Muzyka, in: Superalloys II, 1987, p. 165.
[21] B.P. Miglin, M.T.M., J.V. Monter, T. Sato, K. Aoki, in: Proceedings of the 4th International Conference on Environmental Degradation of Materials in Nuclear Power Systems – Water Reactors, Jekyll Island, Georgia, August 6–10, 1989 (NACE), p. 11.